Aureobasidins: Structure−Activity Relationships for the Inhibition of the Human *MDR1* P-Glycoprotein ABC-Transporter

Françoise Tiberghien,[†,‡] Toru Kurome,[§] Kazutoh Takesako,[§] Agnès Didier,[†] Tom Wenandy,[†] and Francis Loor*[,†]

Laboratory of Immunology, Strasbourg 1 University, BP24, F-67401 Illkirch, France, and Biotechnology Research Laboratories, Takara Shuzo Company, Ltd., 3-4-1 Otsu, Shiga 520-21, Japan

Received November 24, 1999

Cyclic depsipeptide cyclo-[D-Hmp[1]-L-MeVal[2]-L-Phe[3]-L-MePhe[4]-L-Pro[5]-L-aIle[6]-L-MeVal[7]-L-Leu[8]-L-βHOMeVal[9]], the antifungal antibiotic aureobasidin A (AbA), was reported to interfere with ATP-binding cassette (ABC) transporters in yeast and mammalian cells, particularly the *MDR1* P-glycoprotein (Pgp), a transmembrane phospholipid flippase or "hydrophobic vacuum cleaner" that mediates multidrug resistance (MDR) of cancer cells. In a standardized assay that measures Pgp function by the Pgp-mediated efflux of the calcein-AM Pgp substrate and uses human lymphoblastoid MDR-CEM (VBL^{100}) cells as highly resistant Pgp-expressing cells and the cyclic undecapeptide cyclosporin A (CsA) as a reference MDR-reversing agent (IC_{50} of 3.4 μM), AbA was found to be a more active Pgp inhibitor (IC_{50} of 2.3 μM). Out of seven natural analogues and 18 chemical derivatives of AbA, several were shown to display even more potent Pgp-inhibitory activity. The Pgp-inhibitory activity was increased about 2-fold by some minor modifications such as those found in the naturally occurring aureobasidins AbB ([D-Hiv[1]]-AbA), AbC ([Val[6]]-AbA), and AbD [γHOMeVal[9]]-AbA). The replacement of the [Phe[3]-MePhe[4]-Pro[5]] tripeptide by an 8-aminocaprylic acid or the N^7-desmethylation of MeVal[7] led to only a 3.3-fold decreased capacity to inhibit Pgp function, suggesting that the Pgp inhibitory potential of aureobasidins, though favored by the establishment of an antiparallel β-sheet between the [D-Hmp[1]-L-MeVal[2]-L-Phe[3]] and [L-aIle[6]-L-MeVal[7]-L-Leu[8]-] tripeptides, does not critically depend on the occurrence of the [L-Phe[3]-L-MePhe[4]-L-Pro[5]-L-aIle[6]] type II′ β-turn secondary structure. In contrast, the most potent Pgp inhibitors were found among AbA analogues with [βHO-MeVal[9]] residue alterations, with some data suggesting a negative impact of the [L-Leu[8]-L-βHOMeVal[9]-D-Hmp[1]] γ-turn secondary structure on Pgp inhibitory potential. The [2,3-dehydro-MeVal[9]]-AbA was the most potent Pgp inhibitory aureobasidin, being 13-fold more potent than AbA and 19-fold more potent (on a molar basis) than CsA. Finally, there was no correlation between the SAR for the human *MDR1* Pgp inhibition and the SAR for *Saccharomyces cerevisiae* antifungal activity, which is mediated by an inositol phosphoceramide synthase activity.

Introduction

Aureobasidin A (AbA) is an antifungal antibiotic produced by *Aureobasidium pullulans* R106.[1] It is a cyclic depsipeptide containing eight amino acids and a hydroxy acid, with a D-Hmp[1]-MeVal[2]-Phe[3]-MePhe[4]-Pro[5]-aIle[6]-MeVal[7]-Leu[8]-βHOMeVal[9] sequence. This antibiotic (Figure 1) displays interesting structural analogies with the cyclic undecapeptide cyclosporin A (CsA),[2] such as the occurrence of most residues with large hydrophobic side chains and a conformation characterized by a large domain with an antiparallel β sheet, which is critically controlled by specific intramolecular H-bonds involving the amide of some residues and the *N*-methylation of some others.[3−6]

Over 20 minor natural aureobasidin components, named aureobasidin B (AbB) through R (AbR),[3] and five subtypes of AbS[4] have been isolated. AbA and several of its analogues display potent antifungal activity against many pathogenic fungi with low toxicity.[5,6]

AbA was recently shown to be an inhibitor of the *Aur1p* gene-encoded inositol phosphoceramide (IPC) synthase,[7,8] a putative integral membrane protein of the yeast *Saccharomyces cerevisiae* that catalyses the transfer of phosphoinositol from phosphatidylinositol to ceramide to give IPC. Blockade of the phosphoinositol-containing sphingolipid synthesis would inhibit growth and induce cell death of *S. cerevisiae* and other fungi, which unlike mammalian cells contain IPC.

Besides this direct antifungal activity through IPC inhibition, other effects of aureobasidins may be mediated through their interaction with transmembrane proteins which belong to the ATP-binding cassette (ABC) transporter family. One mutant strain of *S. cerevisiae* resistant to aureobasidin (*aur3*) was shown to have a mutation in the pleiotropic drug resistance *PDR1* gene, a transcriptional regulator gene, leading to overexpression of two other genes, the oligomycin resistance gene (*YOR1*) and the pleiotropic drug resistance gene (*PDR5*).[9] Both latter genes encode ABC-transporters, *YOR1* being a member of the cystic fibrosis transmembrane conductance regulator (CFTR) subfamily and *PDR5* being a member of the multiple drug resistance (MDR) subfamily. The possibility that some aureobasidins might also interfere with such fungal

* Corresponding author. Phone: + 33 388 67 69 02. Fax: + 33 388 66 01 90. E-mail: Francis.Loor@pharma.u-strasbg.fr, or loor@aspirine.u-strasbg.fr.
† Strasbourg 1 University.
‡ Present address: EntoMed, Pôle API, Bd Sébastien Brandt, F-67400 Illkirch, France.
§ Takara Shuzo Co.

10.1021/jm990955w CCC: $19.00
Published on Web 06/03/2000

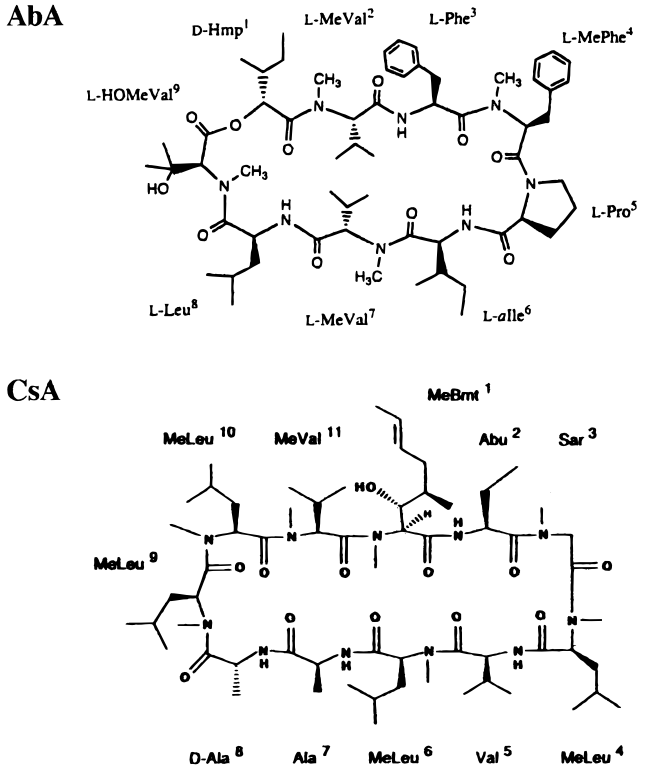

Figure 1. Comparisons of the 2D-structures of aureobasidin A (AbA) and cyclosporin A (CsA). The aureobasidin A (AbA) and cyclosporin A (CsA) structures were adapted from refs 12 and 2, respectively.

ABC-transporters finds some support in the fact that AbA, like CsA, is a substrate of the human *MDR1* P-glycoprotein (Pgp).[10] This 170 kDa plasmamembrane protein acts by effluxing a variety of hydrophobic and ionic compounds, and its overexpression in cancer cells is a major cause of drug resistance. AbA was also shown to interact with human MDR2/3,[10] a CFTR family member expressed in the canalicular liver cells, involved in the phospholipid secretion into the bile.[11] Through such an interference with ABC-transporters, AbA represents a potential cancer MDR-modifying agent, its interference with similar transporters involved in antifungal drug resistance being a more hypothetical perspective.

Previous studies of natural aureobasidins and some chemical derivatives showed different structure−activity relationships for their antifungal activity and their cancer MDR-reversing activity.[12] This distinction between antifungal and MDR-reversing activities was reminiscent of similar data earlier described with *Septoria*-derived cyclopeptolides.[13] Besides the inhibition of Pgp function, reversion of drug resistance may take place at several other levels such as anticancer drug metabolisation by CYP3A. Recently using a standardized calcein-AM assay,[14] which more precisely measures the compound capacity to inhibit Pgp function, we established the structure−activity relationships of cyclosporins for the human *MDR1* Pgp inhibition (unpublished data). The same methodology was applied here with a large number of natural aureobasidins and new chemical derivatives. It suggests that the structure of aureobasidin critical for Pgp inhibition is remarkably polarized to one domain of the molecule.

Chemistry

The natural aureobasidins (molecular weights) AbA (1100), TK-003 (AbB; 1086), TK-004 (AbC; 1086), TK-005 (AbD; 1100), TK-006 (AbE; 1116), TK-007 (AbF; 1086), TK-008 (AbG; 1084), and TK-009 (AbR; 1100) were as described previously.[15]

Other AbA analogues used in this study were all chemically synthesized by three synthetic strategies.

The first strategy was the preparation of analogues by total synthesis as described previously.[16] Six analogues, TK-002 (1024), TK-014 (1100), TK-015 (1100), TK-016 (1100), TK-024 (1087), and TK-025 (1116), were synthesized by this route.

The second strategy was the semisynthetic preparation of analogues using cyclic derivatives TK-010 (1042) and TK-011 (1082), obtained by NaOH treatment of AbA in DMSO and in methanol, respectively.[1,17] Then, oxidation of the olefin of TK-011 with *m*-chloroperbenzoic acid[18,19] in the presence of aluminum chloride in dichloromethane gave an epoxy analogue, TK-012 (unpurified; 1098). The aldol reaction between TK-010 and acetone[17] gave TK-013 (1100), a 1:3.8 mixture of AbA and TK-001 (1100). The diastereomeric ratio was determined by examining the proton NMR signals as described previously.[17]

The third strategy was another semisynthetic strategy used for TK-017 (1106), TK-018 (964), TK-019 (1040), TK-020 (1136), TK-021 (1030), TK-022 (1046), and TK-023 (836). They were prepared by using a linear hexapeptide obtained by chemical digestion of AbA followed by an enzymatical one of the resulting linear nonapeptide.[20] Analogue preparation by the latter strategy (to be detailed elsewhere) will be briefly described here (see Scheme 1).

Briefly, a treatment of AbA with anhydrous hydrogen fluoride (room temperature, 1 h) achieved a diastereoselective opening of AbA,[21] giving a linear nonapeptide [H-L-Phe-L-MePhe-L-Pro-L-aIle-L-MeVal-L-Leu-L-HOMeVal-D-Hmp-L-MeVal-OH] in a 58% yield. After protection of the *N*-terminus amino group of this peptide with a benzyloxycarbonyl (Z) group, the resulting peptide [Z-L-Phe-L-MePhe-L-Pro-L-aIle-L-MeVal-L-Leu-L-HOMeVal-D-Hmp-L-MeVal-OH] was digested at 37 °C with proline-specific endopeptidase,[22] yielding a hexapeptide [H-L-aIle-L-MeVal-L-Leu-L-HOMeVal-D-Hmp-L-MeVal-OH] quantitatively. The Z-protected linear nonapeptide was about 10 times more efficient in the hydrolysis rate as a substrate of the enzyme than the corresponding NH-free one. The *N*-terminus amino group of the linear hexapeptide was then protected with a *tert*-butyloxycarbonyl (Boc) group and the resulting peptide [Boc-L-aIle-L-MeVal-L-Leu-L-HOMeVal-D-Hmp-L-MeVal-OH] was used as the common structural unit for preparation of AbA analogues. A tripeptide, which combined new amino acids at positions 3 and 4 with the Pro at position 5, was coupled with the Boc-protected hexapeptide by the WSCD−HOObt method[23] to give a corresponding nonapeptide without serious racemization of the *C*-terminus amino acid residue of the Boc-hexapeptide, L-MeVal.[2] After usual deprotections, the free linear nonapeptide was afforded to cyclization reaction as described.[16]

The new amino acids of residues 3, 4, 7, and 9 were L-cyclohexylalanine (L-Cha), *N*-methyl-D-phenylalanine

Scheme 1

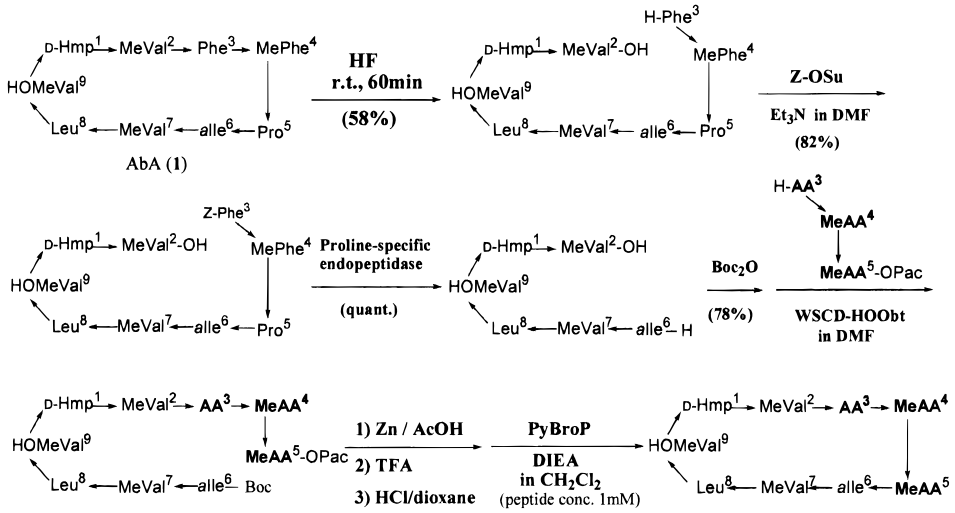

(D-MePhe), L-hydroxyisovaleric acid (L-Hiv), and 2,3-epoxy-*N*-methylvaline (epoxy-MeVal), respectively. For TK-023, the new amino acid replacing residues 3−5 is 8-aminocaprylic acid ($NH(CH_2)_7CO$).

Biological Tests

Cell Lines. A pair of human T-cell leukemia CEM cells, the highly resistant, *MDR1* Pgp-overexpressing MDR-CEM cells (VBL^{100} CEM) and their Pgp-lacking parental Par-CEM cells (CEM 1.3) for controls were maintained at 37 °C in RPMI medium supplemented with 10% FCS, penicillin, and streptomycin, as described earlier.[14]

Cyclic Peptides. All aureobasidins were from Takara Shuzo Co., Ltd, Shiga, Japan. Cyclosporin A (CsA) was from Novartis Pharma Ltd, Basel, Switzerland. The cyclic peptides were dissolved as 10 mg/mL stock solutions and diluted to obtain a range of (3 and 10 stepwise) concentrations in dimethyl sulfoxide (DMSO). They were further diluted in the assay buffer just prior to the test (final 1% DMSO).

P-Glycoprotein (Pgp) Inhibitory Activity. All assays for Pgp activity were performed by use of a standard calcein-AM efflux method with the human leukemia CEM cells, which measures calcein retention.[14] Briefly, Pgp-expressing MDR-CEM cells were first exposed to the Pgp-modulator for 15 min at 37 °C; calcein-AM (0.25 μM final; Molecular Probes Europe BV, Leiden, The Netherlands) was then added, and the cells were kept at 37 °C for a further 15 min. After three cell washes by centrifugation, flicking, and resuspension in the medium, inhibition of Pgp function in Pgp-expressing MDR-CEM cells was measured as calcein specific fluorescence and expressed as the percentage of the calcein retention in Pgp-lacking Par-CEM cells exposed to the same range of Pgp-modulator concentrations. Dose−response correlations were built with the antagonist concentrations on the *X*-axes (log scales) and the percentage of calcein retention in MDR-cells on the *Y*-axes (arithmetic scales). The Pgp-modulator IC_{50} and IC_{20} were the concentrations which, in MDR-CEM cells, restored 50 and 20% of the calcein retention shown by similarly treated Par-CEM cells. With few exceptions, all data are means [± standard deviations (SD)] of three independent experiments (each in duplicates). Cyclosporin A (CsA, a gift from Novartis Pharma Ltd, Basel, Switzerland) was used as reference Pgp inhibitor. Whichever the aureobasidin concentration, the final DMSO content in the assay was 1% (10 μL DMSO/mL medium), with the exception of the 10 μg/mL concentrations of TK-015, TK-016, and TK-021 (3% DMSO); for the latter analogues, the relative Pgp-inhibitory activities were calculated by comparing IC_{20} values (obtained at lower analogue concentrations, with a 1% DMSO content only).

Antifungal Activity. The minimum growth-inhibitory concentrations (MICs) of AbA analogues for *S. cerevisiae* ATCC 9763 were determined by agar dilution method[4−6] using Sabouraud−dextrose agar plates. A loopful of a suspension of a fungi containing approximately 5×10^7 cells/mL was streaked on the surface of the agar plates containing graded concentrations of compounds. After incubation at 30 °C for 3 days, MIC was defined as the lowest compound concentration at which no fungal growth could be detected.

Results

Pgp-Inhibitory Activities. Aureobasidin inhibition of Pgp function was measured by the level of restoration of calcein retention into Pgp-expressing MDR-CEM cells,[14] in comparison with its retention by Pgp-lacking Par-CEM cells and using CsA as reference Pgp inhibitor. AbA was found to be a potent Pgp function inhibitor ($IC_{50} = 2.27 \pm 0.55$ μM; $n = 10$), more active than CsA ($IC_{50} = 3.41 \pm 0.55$ μM; $n = 5$), with no effect on the Pgp-lacking cells. In further experiments, several AbA analogues were found to display a large Pgp-inhibitory activity using the same assay with the same Pgp-expressing cells (Table 1), while lacking effects on Pgp-lacking Par-CEM cells used as controls [no alteration of calcein retention at all testable concentrations (not shown)].

Table 1 reports AbA analogues with single alterations from residue 1 to residue 9, as well as analogues with multiple alterations. The data are shown as IC_{50} and IC_{20} values, and their Pgp inhibitory potency is also shown in comparison to AbA as fold increase ("x") or fold decrease ("/") calculated as ratios of analogue IC_{50} to AbA IC_{50} (or the IC_{20} ratios in a few cases). The structural alterations of aureobasidins will now be

Table 1. Aureobasidin Residue Alterations and Human *MDR1* Pgp Inhibitory Activity[a]

no. TK-	aureobasidin analogue	$IC_{50} \pm SD$ (n) (μM)	$IC_{20} \pm SD$ (n) (μM)	potency vs AbA[b]
AbA		2.27 ± 0.55 (10)	0.68 ± 0.18 (10)	=1
003 (AbB)	[D-Hiv^1]-AbA	1.10 ± 0.06 (3)	0.34 ± 0.02 (3)	**x 2.1**
017	[L-Cha^3]-AbA	5.88 ± 2.71 (2)	1.45 ± 0.45 (4)	/ 2.1
006 (AbE)	[βHOMePhe^4]-AbA	2.15 ± 0.00 (2)	0.81 ± 0.18 (2)	x 1.1
002	[D-MeAla^4]-AbA	4.79 ± 0.49 (3)	1.37 ± 0.10 (3)	/ 2.1
014	[D-MePhe^4]-AbA	2.73 ± 0.59 (3)	0.91 ± 0.18 (3)	/ 1.2
021	[L-Cha^3,D-MeAla4]-AbA	>2.91 (3)	1.17 ± 0.10 (3)	/ 1.7
022	[L-Cha^3,D-MeSer^4]-AbA	5.16 ± 0.38 (3)	2.68 ± 0.57 (3)	/ 2.3
018	[L-Ser^3,D-MeAla^4]-AbA	> 31 (2)	> 31 (2)	/ > 46
019	[L-Tyr^3,D-MeAla^4]-AbA	5.77 ± 0.96 (3)	2.12 ± 0.77 (3)	/ 2.5
020	[L-Tyr(Chm)^3,D-MeAla^4]-AbA	2.11 ± 0.62 (3)	0.64 ± 0.13 (3)	x 1.1
015	[D-Pro^5]-AbA	> 2.73 (3)	1.36 ± 0.27 (3)	/ 2.0
023	[-NH(CH$_2$)$_7$CO-^{3,4,5}]-AbA	7.42 ± 1.07 (3)	2.63 ± 0.36 (3)	/ 3.3
004 (AbC)	[Val^6]-AbA	1.29 ± 0.29 (3)	0.41 ± 0.09 (3)	**x 1.8**
007 (AbF)	[Val^7]-AbA	7.55 ± 0.00 (2)	2.67 ± 0.74 (2)	/ 3.3
016	[D-MeVal^7]-AbA	> 2.73 (3)	1.80 ± 0.18 (3)	/ 2.7
024	[L-Hiv^7]-AbA	1.66 ± 0.39 (3)	0.46 ± 0.06 (3)	**x 1.4**
025	[L-Glu^8]-AbA	> 8.96 (3)	> 8.96 (3)	/ >13
008 (AbG)	[MeVal^9]-AbA	2.68 ± 0.55 (3)	0.69 ± 0.09 (3)	/ 1.2
005 (AbD)	[γHOMeVal^9]-AbA	1.09 ± 0.18 (3)	0.36 ± 0.01 (3)	**x 2.1**
010	[Sar^9]-AbA	0.89 ± 0.03 (2)	0.31 ± 0.01 (2)	**x 2.6**
011	[2,3-dehydro-MeVal^9]-AbA	0.18 ± 0.02 (4)	0.06 ± 0.01 (4)	**x 12.6**
012	[2,3-epoxy-MeVal^9]-AbA (crude)	1.55 ± 0.18 (3)	0.46 ± 0.05 (3)	**x 1.5**
001	[D-βHOMeVal^9]-AbA	0.39 ± 0.08 (3)	0.10 ± 0.01 (3)	**x 5.8**
013	[DL-βHOMeVal^9]-AbA (D/L 3.8:1)	0.36 ± 0.04 (3)	0.10 ± 0.01 (3)	**x 6.3**
009 (AbR)	[βHOMePhe^4, MeVal^9]-AbA	1.36 ± 0.04 (3)	0.46 ± 0.05 (3)	x 1.7

[a] Data are shown as mean inhibitory concentrations (μM) ± standart deviation (n = number of independent experiments). Cha, cyclohexylalanine; Chm, cyclohexylmethyl; Hiv, 2-hydroxyisovaleric acid. The names of the natural analogues are in parentheses. [b] Potency versus AbA. The relative Pgp-inhibitory activities were calculated by comparing the μM IC_{50} values, except for TK-015, TK-016, TK-017, TK-018, TK-021, and TK-025 (used IC_{20} values). Shown in bold are the relative potencies of analogues that inhibit Pgp function substantially more than AbA.

described for each of the eight tested AbA residues (no AbA variant was available for the second residue, L-MeVal^2). The consequences for Pgp-inhibitory activity will be studied with regard to AbA in the case of single modifications or by comparison with the nearest aureobasidin derivatives tested in the case of multiple alterations.

L-Hmp^1. In the naturally occurring AbB, the change of L-Hmp^1 (2-hydroxy-3-methylpentanoic acid) to the smaller L-Hiv^1 [2-hydroxyisovaleric acid = 2-hydroxy-3-methylbutanoic acid (Hmb)] enhanced 2-fold the Pgp-inhibitory activity.

L-Phe^3. The Pgp-inhibitory capacity was decreased more than 2-fold by the change of the aromatic L-Phe^3 (AbA) for the more hydrophobic L-Cha^3 (TK-017). The large variability of the measured IC_{50} values (n = 2), possibly due to solubility problems at high concentration in the assay, led us to rather use the less variable IC_{20} values (n = 4) for further comparisons.

L-MePhe^4. In the naturally occurring AbE, the β-hydroxylation of L-MePhe^4 into L-βHOMePhe^4 did not change Pgp-inhibitory activity. Among the chemical derivatives, the L- to D-isomerization of L-MePhe^4 had surprisingly little effect, with only a slightly reduced Pgp-inhibitory activity (TK-014). Yet, the replacement of L-MePhe^4 by a residue with a smaller side chain (D-MeAla^4) in TK-002 caused a 2-fold decrease of Pgp-inhibitory activity.

L-Phe^3 and L-MePhe^4. Some chemical derivatives, but none of the natural aureobasidins, combined alterations of the third and fourth residues, whose effects on Pgp-inhibitory activity were analyzed in two steps.

[L-Phe^3] Variants of [D-MeAla^4]-AbA Derivatives. With regard to [D-MeAla^4]-AbA (TK-002), the replacement of L-Phe^3 by L-Cha^3 (TK-021) would not change the Pgp-inhibitory activity, as evaluated by the IC_{20} values (IC_{50} could not be measured). In contrast, its replacement by L-Ser^3 (TK-018) led to a complete loss of Pgp-inhibitory activity, presumably due to the substitution of an hydrophobic residue by a polar one.

The L-Phe^3 replacement by L-Tyr^3 (TK-019) only caused a small decrease of Pgp-inhibitory activity (TK-019 IC_{20} values of 2.12 μM instead of 1.37 μM for TK-002), which if significant might be due to the hydroxyl group of Tyr (as found with other cyclic peptides[13]). The derivatization of TK-019 at the hydroxyl of its Tyr^3 seemed to have the expected beneficial effect, since L-Tyr(Chm)^3 (TK-020) showed a substantial Pgp-inhibitory activity that was even 2-fold larger than the one shown by its L-Phe^3-using parent compound (TK-002), restoring a Pgp-inhibitory capacity similar to that of AbA. The combination of [L-Tyr(Chm)^3] and [D-MeAla^4] might stabilize the aureobasidin conformation, improving its capacity for membranous insertion and encounters with Pgp molecules, though the aforementioned residue combination might not itself belong to the aureobasidin residues which actually bind to the Pgp molecules.

Analysis of Residue 4 Alterations with Regard to [L-Cha^3]-AbA (TK-017). By comparing the IC_{20} values with regard to [L-Cha^3]-AbA (TK-017 IC_{20} = 1.45 μM), the replacement of L-MePhe^4 by a D-MeSer^4 decreased the Pgp-inhibitory activity (TK-022 IC_{20} = 2.68 μM), whereas its replacement by D-MeAla^4 might slightly increase the Pgp-inhibitory activity (TK-021 IC_{20} = 1.17 μM).

L-Pro^5. The L- to D-isomerization of L-Pro^5 did not abrogate the Pgp-inhibitory activity, though [D-Pro^5]-AbA was 2-fold less potent than AbA by IC_{20} value comparisons (TK-015 IC_{20} = 1.36 μM).

[L-Phe^3-L-MePhe^4-L-Pro^5]. The replacement of the normal aureobasidin sequence -L-Phe^3-L-MePhe^4-L-Pro^5- by an 8-aminocaprylic acid (-NH(CH_2)$_7$CO-^{3,4,5}) in TK-023 provides a cyclic compound which surprisingly maintained a substantial Pgp-inhibitory activity (only 3.3-fold lower than that of AbA). Together with the results of the other residue alterations at positions 3, 4, and 5, this suggests that this section of the cyclic peptide is not essential for, or not directly involved in, the interaction with Pgp molecules. Yet, substitutions in this area of the molecule may affect other prerequisite factors for efficient interaction with Pgp molecules, such as adequate insertion and diffusion within the plasma-membrane of the Pgp-expressing cells.

L-aIle^6. In the naturally occurring AbC, the L-aIle^6 replacement by the smaller L-Val^6 residue (TK-004) substantially increased the Pgp-inhibitory activity (nearly 2-fold).

L-MeVal^7. The L- to D-isomerization giving D-MeVal^7 (TK-016) did not abolish the capacity to inhibit Pgp function, though substantially reducing it. The naturally occurring AbF (TK-007) showed a L-MeVal^7 *N*-des-methylation, leading to a marked (3.3-fold) decreased Pgp-inhibitory activity. Interestingly, the change of the peptide bond of L-MeVal^7 to a peptolidic bond in L-Hiv^7 (TK-024) did not decrease the Pgp-inhibitory activity and might even favor it (1.4-fold increase).

L-Leu^8. The replacement of L-Leu^8 by L-Glu^8 (TK-025) led to a complete loss of Pgp-inhibitory activity, a feature most likely due to the acid function, as classicaly found with Pgp-inhibitory cyclic peptides.[13]

L-βHOMeVal^9. Alterations of the ninth residue occur in three natural aureobasidins either alone (AbD and AbG) or in combination with another residue alteration (AbR), and interestingly enough this ninth residue seems to have a critical impact on the capacity of aureobasidin to inhibit Pgp function.

The dehydroxylation of L-βHOMeVal^9 in AbG (TK-008; L-MeVal^9) did not significantly change the Pgp-inhibitory activity. Similarly, the crude epoxy form of AbA (TK-012; 2,3-epoxy-MeVal^9) was only slightly more potent than AbA for Pgp inhibition.

In the natural AbD (TK-005), the γ-hydroxylation of L-MeVal^9 instead of its β-hydroxylation (AbA) led to a 2-fold increased Pgp-inhibitory activity.

The L- to D-conversion into D-βHOMeVal^9 (TK-001), even if not complete (D/L ratio of 3.8:1; TK-013) led to a dramatic (about 6-fold) enhancement of Pgp-inhibitory activity.

Remarkably, the replacement of L-βHOMeVal^9 by the simpler Sar^9 residue (TK-010) which maintains the *N*-methylated feature but lacks a side chain, did not decrease but substantially (2.6-fold) increased Pgp-inhibitory activity.

Nevertheless, the most potent Pgp inhibitory aureobasidin was obtained by dehydrogenation of L-βHOMeVal^9 into 2,3-dehydro-MeVal^9 (TK-011). With an IC_{50} of 0.18 $\pm$ 0.02 μM, TK-011 was nearly 13-fold more potent than the parent AbA molecule. The complete dose−response curves for Pgp inhibition by AbA and [2,3-dehydroMeVal^9]-AbA (TK-011) are shown in reference to CsA (Figure 2).

L-MePhe^4 and L-βHOMeVal^9. The naturally occurring AbR (TK-009) cumulates changes at position 4, where it has a L-βHOMePhe^4 like AbE, and at position 9, where it has a L-MeVal^9 like AbG; these together led to 1.7-fold increased Pgp-inhibitory activity, in comparison with AbA.

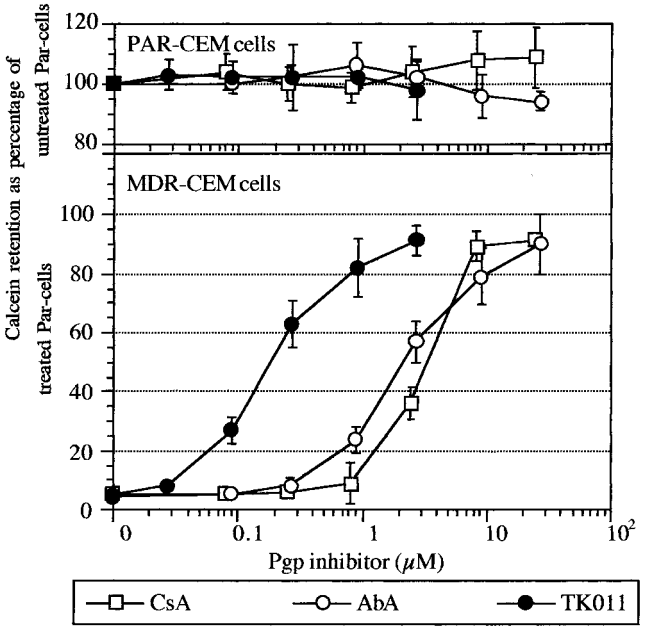

Figure 2. Dose-dependence of Pgp inhibition by AbA, [2,3-dehydro-MeVal^9]-AbA, and CsA. The diagram shows the dose-dependent inhibition of Pgp function, as an increasing calcein retention (*Y*-axes) at increasing concentrations of Pgp inhibitor. For the control Pgp-lacking Par-CEM cells (top part), the levels of calcein retention are expressed as percentages of the levels in Par-CEM cells exposed to 0 μg/mL Pgp inhibitor. For the Pgp-expressing MDR-CEM cells, the restoration of calcein retention is expressed as percentages of the calcein retention shown by similarly treated Par-CEM cells (exposed to the same Pgp inhibitor concentration). Cyclosporin A (CsA, open squares) is used as reference Pgp inhibitor for aureobasidin A (AbA, open circles) and the (TK--011, filled circles). The dose−response curves are means and standard deviations obtained from a minimum of three independent experiments.

In comparison with AbE (TK-006), the sole dehydroxylation of L-βHOMeVal^9 into L-MeVal^9 significantly increased Pgp-inhibitory activity; with AbA, this alteration alone had little effect.

In comparison with AbG (TK-008), the sole β-hydroxylation of L-MePhe^4 into L-βHOMePhe^4 increased Pgp-inhibitory activity about 2-fold; with AbA, this alteration alone had also little effect.

Antifungal Activities. The antifungal data are limited and only shown here for comparison with Pgp-inhibitory activity, as more complete antifungal activities of aureobasidins will be described in an independent paper.[24] All AbA analogues tested for Pgp-inhibitory activity were also studied for antifungal activity with *S. cerevisiae* ATCC9763. Their minimum growth-inhibitory concentrations (MICs) are shown in Table 2, which also provides the AbA/analogue activity ratios.

In this antifungal activity assay, the reference AbA MIC was 0.4 μg/mL and its analogues were generally less active. Only one semisynthetic AbA analogue (TK-014) was more active (2-fold), and only three other AbA analogues, two natural ones (AbB and AbC) and one semisynthetic one (TK-021), were as active as AbA. Most analogues showed much larger MIC values than AbA, being thus less active than AbA: roughly 2-fold (AbE),

Table 2. Antifungal Effects (anti-*S. cerevisiae* Activity) of Aureobasidins[a]

		antifungal activity		
no. TK-	aureobasidin analogue	MIC (μg/mL)	AbA/analogue ratio	Pgp[b] AbA/analogue ratio
AbA		0.4	= 1	=1[a]
003 (AbB)	[D-Hiv^1]-AbA	0.4	1	**2.1**
017	[L-Cha^3]-AbA	1.6	0.25	0.5
006 (AbE)	[βHOMePhe^4]-AbA	0.8	0.5	1.0
002	[D-MeAla^4]-AbA	1.6	0.25	0.5
014	[D-MePhe^4]-AbA	0.2	2	0.8
021	[L-Cha^3,D-MeAla^4]-AbA	0.4	1	0.6
022	[L-Cha^3,D-MeSer^4]-AbA	1.6	0.25	0.5
018	[L-Ser^3,D-MeAla^4]-AbA	>25	<0.016	<0.1
019	[L-Tyr^3,D-MeAla^4]-AbA	25	0.016	0.4
020	[L-Tyr(Chm)^3,D-MeAla^4]-AbA	1.6	0.25	1.0
015	[D-Pro^5]-AbA	1.6	0.25	0.5
023	[-NH(CH$_2$)$_7$CO-^{3,4,5}]-AbA	>25	<0.016	0.4
004 (AbC)	[Val^6]-AbA	0.4	1	**1.8**
007 (AbF)	[Val^7]-AbA	1.6	0.25	0.3
016	[D-MeVal^7]-AbA	>25	<0.016	0.4
024	[L-Hiv^7]-AbA	>25	<0.016	**1.4**
025	[L-Glu^8]-AbA	>25	<0.016	<0.1
008 (AbG)	[MeVal^9]-AbA	>25	<0.016	0.9
005 (AbD)	[γHOMeVal^9]-AbA	6.3	0.06	**2.1**
010	[Sar^9]-AbA	>25	<0.016	**2.7**
011	[2,3-dehydro-MeVal^9]-AbA	>25	<0.016	**12.5**
001	[D-βHOMeVal^9]-AbA	>25	<0.016	**5.8**
009 (AbR)	[βHOMePhe^4, MeVal^9]-AbA	1.6	0.25	**1.7**

[a] Antifungal data are shown as minimum growth-inhibitory concentrations (MIC). For other abbreviations, see Table 1. [b] Potency versus AbA. To provide a direct comparison with antifungal activities, the relative Pgp-inhibitory potencies were calculated here by comparing μg/mL IC_{50} (or IC_{20}) values using the same experimental data as in Table 1. The data for TK-012 and TK-013 were omitted, as they were not available for the antifungal activity. Shown in bold are the relative potencies of analogues that inhibit Pgp function substantially more than AbA.

4-fold (seven analogues, AbF, AbR, TK-002, TK-015, TK-017, TK-020, TK-022), 16-fold (AbD), or over 50-fold (all others). To facilitate the comparisons of antifungal SAR and Pgp inhibition SAR (see Discussion), similarly calculated AbA/analogue activity ratios (based on μg/mL IC_{50} comparisons) are shown for Pgp activity.

Discussion

The present data confirm the earlier reported lack of correlation between the SAR for the human *MDR1* Pgp inhibition and the SAR for *S. cerevisiae* antifungal activity.[12] The lack of correlation is now extended to a larger number of aureobasidins and by use of a method which directly measures *MDR1* Pgp function rather than a reversion of a cancer cell MDR phenotype.

More specifically, this is shown by the comparison of the five analogues with a modified amino acid residue at position 9 (TK-001, -005, -008, -010, and -011): they lost antifungal activity but not Pgp-inhibitory activity; on the contrary, all but TK-008 gained increased Pgp-inhibitory activity. Thus, the amino acid residue at position 9 is very important for both activities, but the structural requirements for its side chain are different for each activity.

Another obvious lack of correlation between the two activities is shown by residue alterations at the third and fourth positions. These residues are important for both inhibitory activities since [L-Ser^3,D-MeAla^4]-AbA lost both activities, and since recovery of Pgp-inhibitory activity together with some increase of antifungal activity can be obtained by replacement of L-Ser^3 with L-Tyr(Chm)^3 or L-Cha^3 to add hydrophobicity. However, [NH(CH$_2$)$_7$CO^{3,4,5}]-AbA retained Pgp-inhibitory activity while having no antifungal activity, and [D-MePhe^4]-AbA, the single AbA analogue with higher antifungal activity than AbA, remained only as active as AbA for *MDR1* Pgp inhibition.

Along the same lines, three different alterations of the seventh residue (L- to D-isomerization, *N*-desmethylation, and peptidic to peptolidic linkage to the eighth residue) were always though variably deleterious for the antifungal activity in the *S. cerevisiae* assay, but they ranged from deleterious to beneficial for Pgp-inhibitory activity. Thus, the conformational requirements of aureobasidins for the antifungal activity and for the Pgp-inhibitory activity are obviously different.

Most structural variations of AbA led to a much lower antifungal activity, with a few exceptions showing an unchanged activity (AbB, AbC, and TK-021) and only one leading to an increased activity (TK-014). Since no antifungal activity was detectable in nearly half of the analogues tested here, a more thorough disclosure of SAR for antifungal activity may come from a broader study of aureobasidin analogues.[24] However, some SAR features can be established here for the inhibition of *MDR1* Pgp function, as both structural alterations increasing this activity and others decreasing it could be found.

Naturally Occurring Aureobasidins. AbA and several of its natural analogues thus showed potent Pgp-inhibitory activity. With an IC_{50} of 2.3 μM, AbA was found to be more active than the reference cyclic undecapeptide CsA (IC_{50} of 3.4 μM). Among the other natural aureobasidins tested, AbB (D-Hiv^1 instead of D-Hmp^1), AbC (Val^6 instead of aIle^6), and AbD (γ-HOMeVal^9 instead of β-HOMeVal^9) were nearly 2-fold more active than AbA. AbA, AbE (β-HOMePhe^4 instead of MePhe^4), and AbG (MeVal^9 instead of β-HOMeVal^9) showed the same Pgp-inhibitory activities, suggesting little importance of these hydroxyl groups for the

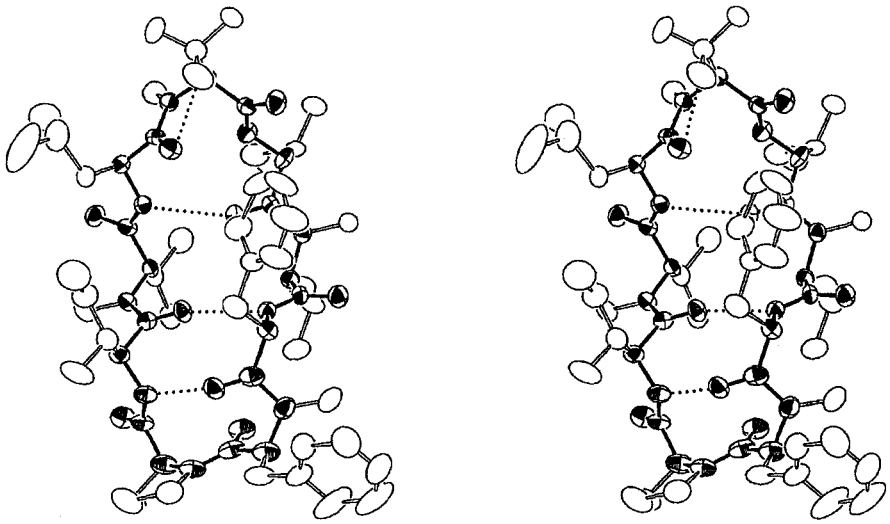

Figure 3. Stereoscopic view of aureobasidin A conformers. The backbone chain is represented by the detailed thermal ellipsoids and thick bonds. Intramolecular hydrogen bonds are shown by dotted lines. Hydrogen atoms were omitted for clarity. The residues are shown clockwise, with [L-βHOMeVal^9] at the top of the molecule, [D-Hmp^1-L-MeVal^2-L-Phe^3-L-MePhe^4] on the right side from top to bottom, and [L-Pro^5-L-aIle^6-L-MeVal^7-L-Leu^8-] on the left side from bottom to top. The transannular H-bonds are (aIle^6)-NH···O=C(Phe^3), (Phe^3)NH···O=C(aIle^6), and (Leu^8)NH···O=C(Hmp^1), as well as between the hydroxyl group of βHOMeVal^9 and the O=C moieties of Leu^8. Reproduced from ref 28 (Copyright 1999).

interaction with Pgp molecules (further discussed below), although the hydroxyl group of the β-HOMeVal^9 was shown to be essential for the antifungal activity.[12] Curiously, AbR was nearly 2-fold more active than AbA, although it combined βHOMePhe^4 and MeVal^9 residues, two modifications which independently did not significantly change the Pgp-inhibitory activity in neither AbE (βHOMePhe^4) nor AbG (MeVal^9). Since both modifications were localized at the two opposite extremities of the cyclic peptolide, an intermolecular H-bond in a head-to-tail fashion, similar to what was found with other peptides,[27] could be implicated in a conformational change improving the Pgp-inhibitory activity. Finally, like in an earlier report,[12] AbF (Val^7 instead of MeVal^7) was the sole natural aureobasidin to be markedly less active than AbA.

The solid-state conformation of AbA obtained by X-ray diffraction analysis (Figure 3) shows an arrowhead-like or elongated pentagon-like conformation with the βHOMeVal^9 residue at the tip.[28]

Like CsA, the backbone conformation of aureobasidin [D-Hmp^1-MeVal^2-Phe^3-MePhe^4-Pro^5-aIle^6-MeVal^7-Leu^8-βHOMeVal^9] can be divided into three types of secondary structures.[25−28]

The [Phe^3-βHOMePhe^4-Pro^5-aIle^6] forms a type II′ β-turn structure, whereas the [Leu^8-βHOMeVal^9-Hmp^1] sequence forms a γ-turn structure with an H-bond between the hydroxyl group of βHOMeVal^9 and the O=C moieties of Leu^8 and an electrostatic short contact of (Hmp^1)=O···N−(βHOMeVal^9).[26−28] The [Hmp^1-MeVal^2-Phe^3] and [aIle^6-MeVal^7-Leu^8] sequences form an antiparallel β-sheet structure stabilized by three transannular hydrogen bonds: (aIle^6)NH···O=C(Phe^3), (Phe^3)NH···O=C(aIle^6), and (Leu^8)NH···O=C(Hmp^1).

Since the only difference between AbF and AbA is an *N*-desmethylation (Val^7 instead of MeVal^7), the deleterious effect on Pgp-inhibitory capacity might come from a modification of the molecule folding by a perturbation of the intramolecular H-bond and the subsequent disruption of the β sheet (further discussed below).

Chemically Modified Aureobasidins. Besides these natural aureobasidins, other chemically modified derivatives were tested, which incorporate one or more modifications, whose analyses may be focused on three domains of the aureobasidin molecule: the tripeptide 3−5, the residue 7, and the residue 9.

The Tripeptide [Phe^3-MePhe^4-Pro^5]. None of the tested modifications of residues 3, 4, and 5 increased the Pgp-inhibitory activity. Even the replacement of L-MePhe^4 by its enantiomer D-MePhe^4 had little effect on activity, despite the fact that it probably stabilizes the β-turn conformation (as suggested by NMR studies of [D-MePhe^4]-AbA). However, replacement of L-MePhe^4 by D-MeAla^4 decreased 2-fold the Pgp-inhibitory activity, suggesting that the latter depended more on the hydrophobicity than on the 3D-orientation of the side chain at position 4.

For two derivatives with a polar Ser residue replacing a Phe residue, the consequence for Pgp inhibition markedly depended on whether position 3 or 4 was concerned. While a Phe to Ser mutation at the fourth position totally destroyed the Pgp-inhibitory activity, it did not dramatically affect it when occurring at the third position (the [L-Cha^3-D-MeSer^4] analogue being only slightly less active than the [L-Cha^3-L-MePhe^4] one). Such differences might be explained in various ways. For instance, the Ser hydroxyl group cannot be involved in an intramolecular H-bond and/or is more exposed to the solvent in the L-Ser^3 residue case than in the D-MeSer^4 one, creating a more hydrophilic surface on that aureobasidin domain which would not favor its retention within the plasma membrane. These comparisons of the impact of the presence of Ser at positions 3 and 4 are however impaired by the fact that one of the compared pairs uses [L-Cha^3] derivatives, and that the replacement of L-Phe^3 by L-Cha^3 caused a clear decrease of activity.

A very informative derivative was obtained by the complete replacement of the [Phe^3-MePhe^4-Pro^5] tripeptide by an 8-aminocaprylic acid (NH(CH$_2$)$_7$CO se-

quence), since it resulted in only a 3.3-fold decreased capacity to inhibit Pgp function in comparison to AbA. This major modification results in a cyclic peptoid with the same number of backbone atoms as AbA, which should allow retention of the second H-bond between (Phe^3)NH···O═C(aIle^6), but is obviously devoid of the side chains of residues 3, 4, and 5. Therefore, Pgp inhibition does not critically depend on those side chains nor on the secondary β-turn type II′ structure of AbA.

The [L-MeVal^7] Residue. Opposite to what was seen with the L- to D-isomerization of the Phe^4 residue, the replacement of L-MeVal^7 by a D-MeVal^7 markedly decreased the Pgp-inhibitory activity, suggesting that the orientation of this side chain was critical for maintaining the activity. However, a distorted or disrupted antiparallel β-sheet of AbA may occur in [residue^7]-modified AbA analogues. Indeed, in the case of the [D-MeVal^7]-AbA, an ^{1}H NMR spectrum indicates the disruption of intramolecular hydrogen bonds in the [D-MeVal^7]-AbA molecule (unpublished data). Similarly, the decreased Pgp-inhibitory activity which was observed by the *N*-desmethylation of L-MeVal^7, as is naturally occurring in AbF ([L-Val^7]-AbA), may also result from a distortion of the AbA conformation. From current analyses of the ^{1}H NMR spectrum and NH proton exchange experiments with D_2O, the conformational alterations caused by the lack of N^7-methyl led to a novel, yet uncompletely resolved aureobasidin conformation, involving the NH protons of L-Val^7 and of at least one of the L-Phe^3, L-aIle^6, and L-Leu^8 residues (unpublished data). The results suggest that, besides the usual arrowhead conformation typical of AbA, AbF may acquire an unknown conformation with a distorted β-sheet or arrowhead, with deleterious effects on both Pgp inhibitory and antifungal activities. Interestingly, another [residue^7]-AbA analogue obviously unable to provide either a N^7-methyl or a N^7-H proton ([L-Hiv^7]-AbA) could inhibit Pgp function slightly more (1.4-fold) than AbA, but showed a 4.5-fold larger Pgp-inhibitory activity than AbF ([L-Val^7]-AbA). This also suggests that the potential for H-bonding involving the amide of the L-Val^7 residue may be actually responsible for the decreased Pgp inhibitor activity of AbF.

Recent X-ray crystallographic studies of AbA and molecular modeling of the possible effects of amide *N*-desmethylation suggest that the absence of one, two, three, or all four *N*-methyl moieties leads to different stable but considerably twisted conformations, neither of which shows the arrowhead-like conformation of AbA, especially the γ-turn structure at the [Leu^8-L-βHOMeVal^9-Hmp^1] sequence.[28] It appears that the four *N*-methylated amides (MeVal^2, MePhe^4, MeVal^7, and L-βHOMeVal^9) of AbA and other active antifungal analogues may play an essential role in preserving antifungal activity by restricting the possible conformations of the depsipeptide to the biologically useful ones.[28]

The [L-βHOMeVal^9] Residue. The involvement of the ninth residue of aureobasidins in the Pgp-inhibitory activity is a most obvious feature, since out of six tested AbA analogues with various alterations (including AbR, to be compared with AbE), five conferred an enhanced capacity to inhibit Pgp function, with no change of activity for the last one. More specifically, the [2,3-dehydro-MeVal^9]-AbA derivative was nearly 13-fold more active than AbA, 2-fold more active than the [D-βHOMeVal^9]-AbA analogue, and 5−6-fold more active than the simpler [Sar^9]-AbA chemical analogue or the natural AbD ([L-γHOMeVal^9]-AbA). In contrast to an earlier report,[12] the hydroxyl group was not found to be essential for the Pgp-inhibitory activity, the natural AbG ([L-MeVal^9]-AbA) being not significantly less active than AbA. All together, the Pgp-inhibitory activities shown by several ninth residue analogues of AbA suggest that, in contrast to its requirement for the antifungal activity, the aforementioned γ-turn structure formed by the [Leu^8-L-βHOMeVal^9-D-Hmp^1] sequence found in AbA is not required for expression of Pgp-inhibitory action and might actually impair it.

In view of the very large Pgp-inhibitory activity shown by the 2,3-dehydro-MeVal^9 derivative of AbA, more potent Pgp inhibitors might be obtained by similar chemical modification of AbB ([D-Hiv^1]-AbA) and AbC ([Val^6]-AbA), which, in their native status, were already about 2-fold more active than AbA. However, a recent comparison of the 2,3-dehydro-MeVal^9 derivatives of AbA and AbB showed them to be equipotent: using a new (slightly more resistant) subline of MDR-CEM cells, we obtained identical IC_{50} values for the AbA derivative (MW 1082; $IC_{50} = 0.38 \pm 0.10$ μM,, $n = 3$) and the AbB derivative (MW 1068; $IC_{50} = 0.38 \pm 0.12$ μM, $n = 10$). This suggests that the 2,3-dehydro-MeVal^9 structure dominates the Pgp-inhibitory potential of aureobasidins, whether they have a D-Hmp^1 (AbA) or D-Hiv^1 (AbB) residue, but this might not be extrapolated to AbC (its 2,3-dehydro-MeVal^9 derivative was not available), which shows a smaller Val^6 residue instead of the aIle^6 residue found in AbA.

Since the [2,3-dehydro-MeVal^9]-derivatives of AbA and AbB are very potent Pgp inhibitors, they may have a therapeutic potential for reversal of *MDR1* Pgp-dependent multidrug resistance of cancer. Obviously, a possible interference of chemically modified aureobasidins with ABC-transporters of CFTR subfamily should also be studied. While their inhibitory effect on transporters such as MRP1 might be useful in multidrug resistant cancer treatment, inhibition of other transporters might be deleterious such as an interference with MDR2/3, implicated in the phospholipid secretion into the bile.[10,11]

With regard to the biological activity mechanisms, the Pgp-inhibitory activity of aureobasidins and cyclosporins for eukaryotic cells does not seem to be the only one by which these cyclic peptides may modulate membrane phospholipid metabolism. Both aureobasidins and cyclosporins are also endowed with antifungal activity, and the mechanism used by aureobasidins was recently resolved. Indeed, AbA is an inhibitor of the inositol phosphoceramide (IPC) synthase encoded by the aureobasidin resistance gene *AUR1* isolated from *S. cerevisiae*.[7,8] Some chemical modifications of AbA which increase the Pgp-inhibitory activity wipe out the IPC-synthase inhibitory activity. The activity against *S. cerevisiae* of AbA is caused by the inhibition of IPC synthase, which is essential for growth.[8] SARs for the antifungal activity of cyclosporins have not been reported and the antifungal mechanism of CsA is unclear (e.g. inhibition of the fungus morphogenesis,[29] cytochrome P450 enzymes,[30] calcineurin[31]) and may depend

on the activity of fungal integral membrane transporters such as the FKS1 protein.[32] However, in mammalian cells, cyclosporin was recently found to be involved in the ceramide metabolism as causing an enhanced ceramide production leading to cell apoptosis.[33,34] The mechanism of enhancement appears to be via a synthetic route rather than through the degradation of sphingomyelin by sphingomyelinase.[35] In this case, the more potent inhibition of Pgp function shown by a chemical cyclosporin derivative over CsA[36] interestingly coincided with a larger capacity to increase cellular ceramide formation.[34]

Conclusion

Both aureobasidins and cyclosporins are cyclic peptides with typical "membrane-active agent" features, which share very potent Pgp-inhibitory activity for mammalian cells, suggesting that both are inhibiting the *MDR1* Pgp encoded flippase or "hydrophobic vacuum cleaner". The most common forms of these cyclic peptides, AbA and CsA, display intrinsic Pgp-inhibitory activity, presumably acting as slow Pgp substrates (as the simplest hypothesis). This Pgp-inhibitory activity can be increased by various chemical alterations of both AbA and CsA, which may destroy the other activity of the cyclopeptide, and similarly, minor structural variations which modulate their level of activity for various other enzymes concerned with phospholipid metabolism do not necessarily pair with increased *MDR1* flippase inhibition.

Experimental Section

Abbreviations. Amino acid abbreviations: Abu, α-aminobutyric acid; aIle, allo-isoleucine; Hiv, 2-hydroxyisovaleric acid (=Hmb); Hmb, 2-hydroxy-3-methylbutanoic acid (=Hiv); Hmp, 2-hydroxy-3-methylpentanoic acid; MeBmt, *N*-methyl-4-butenyl-4-methyl-threonine; MeLeu, *N*-methylleucine; MePhe, *N*-methylphenylalanine; MeVal, *N*-methylvaline; Sar, sarcosine. Other abbreviations: AbA−AbS, aureobasidin A−S; ABC, ATP-binding cassette; CsA, cyclosporin A; DMSO, dimethyl sulfoxide; IPC, inositol phosphoceramide; MDR, multiple drug resistance; MDR-, multidrug resistant; MIC, minimum growth-inhibitory concentration; Par-, parental; Pgp, P-glycoprotein.

General Procedures. The three strategies used for the preparation of analogues are described under chemistry. Analogues were purified by preparative TLC or HPLC (ODS). All analogues except for TK-012 (unpurified) were more than 90% pure on HPLC analysis (UV 210 nm). Merck Kieselgel 60 F254 (silica gel, Merck) was used for TLC. Capcell Pak C18 column (Shiseido Co., Ltd.) was used for HPLC. The following spectroscopic and analytical instruments were used: ^{1}H NMR, JEOL JNM-GSX-270 (270 MHz, ref TMS); FAB-MS, JEOL JMS-DX 302.

Analogues Synthesized by the First Strategy. [D-MePhe^4]-AbA (TK-002): Colorless solid; ^{1}H NMR (270 MHz, $CDCl_3$, 3.0 mM, 300 K, only one conformer) δ 8.68 (d, 1H, J = 9.9 Hz), 7.98 (d, 1H, J = 7.3 Hz), 7.52 (d, 1H, J = 8.2 Hz), 7.35−7.10 (m, total 10H), 5.79 (d, 1H, J = 1.3 Hz, Hmp α), 5.36 (d, 1H, J = 11.2 Hz), 5.45 (m, 1H), 4.96 (m, 1H), 4.91 (d, 1H, J = 11.2 Hz), 4.75 (m, 1H), 4.65 (d, 1H, J = 6.6 Hz), 4.56 (t, 1H, J = 9.2 Hz), 4.32 (br s, 1H), 3.44 (s, 3H, N−CH_3), 3.33 (s, 3H, N−CH_3), 3.29 (s, 3H, N−CH_3), 2.85 (s, 3H, N−CH_3), 2.30 (m, 2H), 2.06 (m, 1H), 1.79 (m, 2H), 1.40 (s, 3H), 1.34 (s, 3H); FAB-MS m/z 1101 $[MH]^+$.

[D-MeAla^4]-AbA (TK-014): Colorless powder; ^{1}H NMR (270 MHz, $CDCl_3$, 8.1 mM, 300 K, only one conformer) δ 8.62 (d, 1H, J = 10.2 Hz), 7.95 (d, 1H, J = 7.3 Hz), 7.67 (d, 1H, J = 8.7 Hz), 7.35−7.11 (m, 5H), 5.79 (d, 1H, J = 1.3 Hz, Hmp α), 5.27 (m, 1H), 4.97 (m, 1H), 4.88 (d, 1H, J = 11.2 Hz), 4.30 (br s, 1H), 4.04 (br t, 1H), 3.44 (s, 1H), 3.33 (s, 3H, N−CH_3), 3.32 (s, 3H, N−CH_3), 3.20 (s, 3H, N−CH_3), 3.02 (m, 2H), 2.85 (s, 3H, N−CH_3), 2.45 (m, 1H), 2.27 (m, 2H), 2.02 (m, total 3H), 1.80 (m, 2H), 1.40 (s, 3H), 1.34 (s, 3H), 1.08 (d, 3H, J = 6.6 Hz); FAB-MS m/z 1026 $[MH]^+$, 1048 $[MNa]^+$.

[D-MeVal^7]-AbA (TK-016): Colorless solid; ^{1}H NMR (270 MHz, $CDCl_3$, 3.2 mM, 298 K, only one conformer) δ 7.32−7.02 (m, total 10H), 6.94 (d, 1H, J = 10.3 Hz), 6.71 (d, 1H, J = 10.0 Hz), 6.47 (d, 2H, J = 6.4 Hz), 6.31 (d, 1H, J = 9.5 Hz), 5.38 (s, 1H, Hmp α), 5.17 (m, 1H), 4.97 (m, 1H), 4.86 (d, 1H, J = 5.9 Hz), 4.75 (d, 1H, J = 9.8 Hz), 4.62 (t, 1H, J = 10.3 Hz), 3.09 (s, 3H, N−CH_3), 2.98 (s, 3H, N−CH_3), 2.83 (s, 3H, N−CH_3), 2.45 (s, 3H, N−CH_3), 1.33 (s, 3H); FAB-MS m/z 1101 $[MH]^+$, 1123 $[MNa]^+$.

[-NH(CH$_2$)$_7$CO-^{3,4,5}]-AbA (TK-023): Colorless powder; ^{1}H NMR (270 MHz, $CDCl_3$, 10.0 mM, 300 K, only one conformer) δ 8.25 (d, 1H, J = 7.9 Hz, NH), 6.79 (d, 1H, J = 7.6 Hz, NH), 5.96 (m, 1H), 4.85−4.74 (m, total 2H), 4.71 (m, 1H), 4.58 (d, 1H, J = 9.9 Hz), 2.32 (m, total 4H); FAB-MS m/z 837 $[MH]^+$.

[L-Hmb^7]-AbA (TK-024): Colorless solid; ^{1}H NMR (270 MHz, $CDCl_3$, 7.7 mM, 298 K, only one conformer) δ 8.31 (m, 1H, NH), 8.17 (d, 1H, J = 8.8 Hz, NH), 7.33−7.14 (m total 9H), 6.89 (m, 1H, J = 11.5 Hz), 5.87 (br s, 1H, Hmp α), 5.21 (d, 1H, J = 8.1 Hz), 5.13−4.95 (m, total 3H), 4.78 (m, 1H), 4.42 (d, 1H, J = 11.0 Hz), 4.10 (m, 1H), 3.27 (s, 3H, N−CH_3), 3.12 (s, 3H, N−CH_3), 2.81 (s, 3H, N−CH_3), 2.28 (m, 1H); FAB-MS m/z 1087 $[MH]^+$, 1110 $[MNa]^+$.

Analogues Synthesized by the Second Strategy. [2,3-Dehydro MeVal^9]-AbA (TK-011): Colorless solid; the analytical data of this compound was identical with that described previously.[1]

[2,3-Epoxy-MeVal^9]-AbA (crude) (TK-012): Colorless solid; [2,3-epoxy-MeVal^9]-AbA was detected in 60% purity in TK-012 as determining by HPLC analysis (UV 210 nm); FAB-MS m/z 1099 $[MH]^+$.

Analogues Synthesized by the Third Strategy. [L-Cha^3]-AbA (TK-017): Colorless powder; ^{1}H NMR (270 MHz, $CDCl_3$, 8.6 mM, 300 K, major:minor = 1.2:1) major conformer, δ 7.32−7.29 (m, 3H), 7.17−7.15 (m, 2H), 5.79 (br s, 1H), 5.25−5.01 (m, total 3H), 4.95−4.75 (m, total 2H), 3.29 (s, 3H), 3.16 (s, 3H), 3.13 (s, 3H), 1.25 (s, 10H); FAB-MS m/z 1107 $[MH]^+$, 1129 $[MNa]^+$.

[L-Ser^3,D-MeAla^4]-AbA (TK-018): Colorless solid; ^{1}H NMR (270 MHz, $CDCl_3$, 9.5 mM, 300 K, only one conformer) δ 8.28 (d, 1H, J = 9.6 Hz), 7.65 (d, 1H, J = 6.3 Hz), 7.47 (d, 1H, J = 8.9 Hz), 5.59 (d, 1H, J = 4.3 Hz, Hmp α), 5.27 (m, 1H), 5.16 (d, 1H, J = 11.6 Hz), 4.90−4.67 (m, total 4H), 4.05−3.75 (m, total 3H), 3.39 (s, 1H), 3.30 (s, 3H), 3.29 (s, 3H), 3.28 (s, 3H) and 3.20 (s, 3H), 2.37−2.17 (m, total 3H), 2.01−1.94 (m, total 3H), 1.34 (s, 3H), 1.26 (s, 3H), 1.01 (d, 3H, J = 6.3 Hz); FAB-MS m/z 965 $[MH]^+$, 986 $[MNa]^+$.

[L-Tyr^3,D-MeAla^4]-AbA (TK-019): Colorless solid; ^{1}H NMR (270 MHz, $CDCl_3$, 8.0 mM, 300 K, only one conformer) δ 8.52 (d, 1H, J = 9.9 Hz), 7.89 (d, 1H, J = 6.9 Hz), 7.56 (d, 1H, J = 8.3 Hz), 6.91 (d, 2H, J = 8.6 Hz), 6.81 (d, 2H, J = 8.6 Hz), 5.75 (d, 1H, J = 1.0 Hz, Hmp), 5.40 (d, 1H, J = 11.2 Hz), 5.21 (m, 1H), 5.02 (m, 1H), 4.79 (d, 1H, J = 11.2 Hz), 4.75 (m, 1H), 4.66 (d, 1H, J = 6.6 Hz), 4.54 (d, 1H, J = 8.9 Hz), 4.31 (br s, 1H), 4.06 (m, 1H), 3.37 (s, 3H), 3.32 (s, 3H), 3.23 (s, 3H), 2.73 (s, 3H); FAB-MS m/z 1041 $[MH]^+$, 1062 $[MNa]^+$.

[L-Tyr(Chm)^3,D-MeAla^4]-AbA (TK-020): Colorless powder; ^{1}H NMR (270 MHz, $CDCl_3$, 7.3 mM, 300 K, only one conformer) δ 8.70 (d, 1H, J = 10.1 Hz), 8.07 (d, 1H, J = 7.6 Hz), 7.78 (d, 1H, J = 8.6 Hz), 7.05 (d, 2H, J = 8.6 Hz), 6.85 (d, 2H, J = 8.3 Hz), 5.85 (s, 1H), 5.30 (d, 1H, J = 11.3 Hz), 5.18 (m, 1H), 4.96 (m, total 2H), 4.68 (d, 1H, J = 7.0 Hz), 4.64 (d, 1H, J = 7.3 Hz), 4.58 (t, 1H, J = 9.3 Hz), 4.27 (s, 1H), 4.04 (t, 1H, J = 7.8 Hz), 3.77 (m, 1H), 3.32 (s, 6H), 3.18 (s, 3H), 3.02 (s, 3H); FAB-MS m/z 1137 $[MH]^+$, 1159 $[MNa]^+$.

[L-Cha^3,D-MeAla^4]-AbA (TK-021): Colorless powder; ^{1}H NMR (270 MHz, $CDCl_3$, 8.1 mM, 300 K, only one conformer) δ 8.55 (d, 1H, J = 9.9 Hz), 7.92 (d, 1H, J = 7.6 Hz), 7.75 (d, 1H, J = 8.2 Hz), 5.82 (d, 1H, J = 1.7 Hz, Hmp), 5.24−5.20 (m,

total 2H), 5.00 (d, 1H, J = 10.9 Hz), 4.94 (m, 1H), 4.67 (d, 1H, J = 7.3 Hz), 4.56 (t, 1H, J = 9.2 Hz), 4.03 (m, 1H), 3.29 (s, 3H), 3.28 (s, 3H), 3.27 (s, 3H), 3.24 (s, 3H); FAB-MS *m*/*z* 1030 $[MH]^+$, 1052 $[MNa]^+$.

[L-Cha³,D-MeSer⁴]-AbA (TK-022): Colorless solid; ^{1}H NMR (270 MHz, $CDCl_3$, 8.0 mM, 300 K, only one conformer) δ 8.56 (d, 1H, J = 10.2 Hz), 7.90 (d, 1H, J = 7.6 Hz), 7.76 (d, 1H, J = 8.6 Hz), 5.81 (d, 1H, J = 1.7 Hz), 5.28 (m, 1H), 5.21 (d, 1H, J = 11.6 Hz), 4.98 (d, 1H, J = 10.9 Hz), 4.90 (m, 1H), 4.70−4.56 (m, total 2H), 4.21 (s, 1H), 4.10−4.03 (m, total 2H), 3.39 (s, 3H), 3.29 (s, 3H), 3.26 (s, 3H), 3.23 (s, 3H); FAB-MS *m*/*z* 1047 $[MH]^+$, 1068 $[MNa]^+$.

Acknowledgment. We are very grateful to Prof. T. Ishida, Osaka University of Pharmaceutical Sciences, for his discussion of our AbF conformation analyses. F.T. and A.D. were supported by postdoctoral fellowships (ADRERUS/Strasbourg University). T.W. was supported by postgraduate BPU98/118 and BFR99/024 fellowships (Ministry of Research and Education, Luxembourg) and a 'Legs Kanning' fellowship (Lions International, Luxembourg).

References

(1) Ikai, K.; Takesako, K.; Shiomi, K.; Moriguchi, M.; Umeda, Y.; Yamamoto, J.; Kato, I.; Naganawa, H. Structure of aureobasidin A. *J. Antibiot.* **1991**, *44*, 925−933.
(2) Traber, R. Biosynthesis of cyclosporins. In *Biotechnology of Antibiotics*, 2nd ed.; Strohl, W. R., Ed.; Marcel Dekker Inc.: Basel, 1997; pp 279−313.
(3) Ikai, K.; Shiomi, K.; Takesako, K.; Mizutani, S.; Yamamoto, J.; Ogawa, Y.; Ueno, M.; Kato, I. Structures of aureobasidins B to R. *J. Antibiot.* **1991**, *44*, 1187−1198.
(4) Yoshikawa, Y.; Ikai, K.; Umeda, Y.; Ogawa, A.; Takesako, K.; Kato, I.; Naganawa, H. Isolation, structures, and antifungal activities of new aureobasidins. *J. Antibiot.* **1993**, *46*, 1347−1354.
(5) Takesako, K.; Kuroda, H.; Inoue, T.; Haruna, F.; Yoshikawa, Y.; Kato, I.; Uchida, K.; Hiratani, T.; Yamaguchi, H. Biological properties of aureobasidin A, a cyclic depsipeptide antifungal antibiotic. *J. Antibiot.* **1993**, *46*, 1414−1420.
(6) Endo, M.; Takesako, K.; Kato, I.; Yamaguchi, H. Fungicidal action of aureobasidin A, a cyclic depsipeptide antifungal antibiotic, against *Saccharomyces cerevisiae*. *Antimicrob. Agents Chemother.* **1997**, *41*, 672−676.
(7) Nagiec, M. M.; Nagiec, E. E.; Baltisberger, J. A.; Wells, G. B.; Lester, R. L.; Dickson, R. C. Sphingolipid synthesis as a target for antifungal drugs. Complementation of the inositol phosphorylceramide synthase defect in a mutant strain of *Saccharomyces cerevisiae* by the AUR1 gene. *J. Biol. Chem.* **1997**, *272*, 9809−9817.
(8) Hashida-Okado, T.; Ogawa, A.; Endo, M.; Yasumoto, R.; Takesako, K.; Kato, I. AUR1, a novel gene conferring aureobasidin resistance on *Saccharomyces cerevisiae*: a study of defective morphologies in Aur1p-depleted cells. *Mol. Gen. Genet.* **1996**, *251*, 236−244.
(9) Ogawa, A.; Hashida-Okado, T.; Endo, M.; Yoshioka, H.; Tsuruo, T.; Takesako, K.; Kato, I. Role of ABC transporters in aureobasidin A resistance. *Antimicrob. Agents Chemother.* **1998**, *42*, 755−761.
(10) Kino, K.; Taguchi, Y.; Yamada, K.; Komano, T.; Ueda, K. Aureobasidin A, an antifungal cyclic depsipeptide antibiotic, is a substrate for both human MDR1 and MDR2/P-glycoproteins. *FEBS Lett.* **1996**, *399*, 29−32.
(11) Van Helvoort, A.; Smith, A. J.; Sprong, H.; Fritzsche, I.; Schinkel, A. H.; Borst, P.; Van Meer, G. MDR1 P-glycoprotein is a lipid translocase of broad specificity, while MDR3 P-glycoprotein specifically translocates phosphatidylcholine. *Cell* **1996**, *87*, 507−517.
(12) Kurome, T.; Takesako, K.; Kato, I.; Tsuruo, T. Aureobasidins as new inhibitors of P-glycoprotein in multidrug resistant tumor cells. *J. Antibiot.* **1998**, *51*, 353−358.
(13) Emmer, G.; Grassberger, M. A.; Schulz, G.; Boesch, D.; Gavériaux, C.; Loor, F. Derivatives of a novel cyclopeptolide. 2. Synthesis, activity against multidrug resistance in CHO and KB cells in vitro, and structure−activity relationships. *J. Med. Chem.* **1994**, *37*, 1918−1928.
(14) Tiberghien, F.; Loor, F. Ranking of P-glycoprotein substrates and inhibitors by a calcein-AM fluorometry screening assay. *Anti-Cancer Drugs* **1996**, *7*, 568−578.
(15) Takesako, T.; Ikai, K.; Haruna, F.; Endo, M.; Shimanaka, K.; Sono, E.; Nakamura, T.; Kato, I.; Yamaguchi, H. Aureobasidins, new antifungal antibiotics. Taxonomy, fermentation, isolation, and properties. *J. Antibiot.* **1991**, *44*, 919−924.
(16) Kurome, T.; Inami, K.; Inoue, T.; Ikai, K.; Takesako, K.; Kato, I.; Shiba, T. Total synthesis of an antifungal cyclic depsipeptide Aureobasidin A. *Tetrahedron* **1996**, *52*, 4327−4346.
(17) Rodriguez, M. J.; Zweifel, M. J. Aldol-promoted reaction of R106−Sarcosine: Synthesis and conformational analysis of novel R106 analogues. *J. Org. Chem.* **1996**, *61*, 1564−1572.
(18) Rao, A. S.; Paknikar, S. K.; Kirtane, J. G. Recent advances in the preparation and synthetic applications of oxiranes. *Tetrahedron* **1983**, *39*, 2323−2367.
(19) Rebek, J., Jr. Progress in the development of new epoxidation reagents. *Heterocycles* **1981**, *15*, 517−545.
(20) Kurome, T.; Inoue.; Takesako, K.; Inami, K.; Kato, I. Aureobasidins. US Patent, US 5698670.
(21) Inami, K.; Kurome, T.; Takesako, K.; Kato, I.; Shiba, T. Site-specific opening of depsipeptide Aureobasidin A in hydrogen fluoride. *Tetrahedron Lett.* **1996**, *37*, 2043−2044.
(22) Yoshimoto, T.; Walter, R.; Tsuru, D. Proline-specific endopeptidase from *Flavobacterium*. Purification and properties. *J. Biol. Chem.* **1980**, *255*, 4786−4792.
(23) Harrison, D.; Smith, A. C. B. 435. The synthesis of some cyclic hydroxamic acids from O-aminocarboxylic acids. *J. Chem. Soc.* **1960**, 2157−2160.
(24) Kurome, T.; Takesako, K.; et al. Manuscript in preparation.
(25) Fujikawa, A.; In, Y.; Urata, H.; Inoue, M.; Ishida, T.; Nemoto, N.; Kobayashi, Y.; Kataoka, R.; Ikai, K.; Takesako, K.; Kato, I. X-ray and NMR conformational study of Aureobasidin E: A cyclic depsipeptide with potent antifungal activity. *J. Org. Chem.* **1994**, *59*, 570−578.
(26) Ikai, K.; Shiomi, K.; Takesako, K.; Kato, I.; Naganawa, H. NMR studies of aureobasidins A and E. *J. Antibiot.* **1991**, *44*, 1199−1207.
(27) Okuyama, K.; Ohuchi, S. Recent structural studies of peptides in Japan. *Biopolymers* **1996**, *40*, 85−103.
(28) In, Y.; Ishida, T.; Takesako, K. Unique molecular conformation of aureobasidin A, a highly amide-*N*-methylated cyclic depsipeptide with potent antifungal activity: X-ray crystal structure and molecular modeling studies. *J. Pept. Res.* **1999**, *53*, 492−500.
(29) Sazykin, Y. O., Telesnina, G. N.; Zaslavskaya, P. L.; Krakhmaleva, I. N.; Bibikova, M. V.; Rybakova, A. M.; Ivanitskaya, L. P.; Vavashin, S. M. Cyclosporin effect on certain metabolic processes in fungi. *Antibiot. Khimiother.* **1994**, *39*, 3−9.
(30) Lomaestro, B. M.; Piatek, M. A. Update on drug interactions with azole antifungal agents. *Ann. Pharmacother.* **1998**, *32*, 915−928.
(31) Odom, A.; Muir, S.; Lim, E.; Toffaletti, D. L.; Perfect, J.; Heitman, J. Calcineurin is required for virulence of *Cryptococcus neoformans*. *EMBO J.* **1997**, *16*, 2576−2589.
(32) Eng, W. K.; Faucette, L.; McLaughlin, M. M.; Cafferkey, R.; Koltin, Y.; Morris, R. A.; Young, P. R.; Johnson, R. K.; Livi, G. P. The yeast FKS1 gene encodes a novel membrane protein, mutations in which confer FK506 and cyclosporin A hypersensitivity and calcineurin-dependent growth. *Gene* **1994**, 61−71.
(33) Bezombes, C.; Maestre, N.; Laurent, G.; Levade, T.; Bettaïeb, A.; Jaffrézou, J. P. Restoration of TNF-α-induced ceramide generation and apoptosis in resistant human leukemia KG1a cells by the P-glycoprotein blocker PSC 833. *FASEB J.* **1998**, *12*, 101−109.
(34) Cabot, M. C.; Han, T. Y.; Giuliano, A. E. The multidrug resistance modulator SDZ PSC 833 is a potent activator of cellular ceramide formation. *FEBS Lett.* **1998**, *431*, 185−188.
(35) Cabot, M. C.; Giuliano, A. E.; Han, T. Y.; Liu, Y. Y. SDZ PSC 833, the cyclosporine A analogue and multidrug resistance modulator, activates ceramide synthesis and increases vinblastine sensitivity in drug-sensitive and drug-resistant cancer cells. *Cancer Res.* **1999**, *59*, 880−885.
(36) Bosch, I.; Dunussi-Joannopoulos, K.; Wu, R. L.; Furlong, S. T.; Croop, J. Phosphatidylcholine and phosphatidylethanolamine behave as substrates of the human *MDR1* P-glycoprotein. *Biochemistry* **1997**, *36*, 5685−5694.

JM990955W